Polymer 50 (2009) 510–518

Contents lists available at ScienceDirect

Polymer

journal homepage: www.elsevier.com/locate/polymer

Synthesis and properties of novel sulfonated polyimides bearing sulfophenyl pendant groups for fuel cell application

Kangcheng Chen, Xinbing Chen, Kazuaki Yaguchi, Noritaka Endo, Mitsuru Higa, Ken-ichi Okamoto*

Graduate School of Science and Engineering, Yamaguchi University, Tokiwadai 2-16-1, Ube, Yamaguchi 755-8611, Japan

ARTICLE INFO

Article history:
Received 7 September 2008
Received in revised form
14 November 2008
Accepted 18 November 2008
Available online 25 November 2008

Keywords:
Sulfonated polyimide
Polymer electrolyte membrane
Polymer electrolyte fuel cell

ABSTRACT

A novel sulfonated diamine bearing sulfophenyl pendant groups, namely, 4,4′-bis (4-aminophenoxy)-3,3′-bis(4-sulfophenyl) biphenyl and a series of sulfonated polyimides (SPIs) based on it were successfully synthesized. The SPIs had high viscosity and gave tough, flexible and transparent membranes. The SPI membranes showed anisotropic membrane swelling in water with 2.5–4 times larger swelling in thickness direction than in plane one. They displayed reasonably high proton conductivity. For example, the conductivities for the SPI with an ion exchange capacity of 1.80 mequiv/g were 104 and 7.3 mS/cm in water and 50% RH, respectively, at 60 °C. They maintained high mechanical strength and proton conductivity even after aging in water at 130 °C for 500 h, showing the high water stability comparable to the best SPI reported so far. In polymer electrolyte fuel cells (PEFCs) operated at 90 °C and 50% RH, they showed fairly high cell performances and have high potential for PEFC applications.

1. Introduction

In recent years, polymer electrolyte fuel cells (PEFCs) have been recognized as one of the most promising energy sources for transportation, stationary and portable devices because of their high energy efficiency and low pollution to environment. Polymer electrolyte membrane (PEM) plays a key role in a PEFC system, namely to separate effectively the anode and cathode gases and to conduct protons under a variety of operating conditions. Currently, perfluorinated ionomers are the state of the art materials because of their excellent chemical stability and high proton conductivity [1,2]. However, high cost, high fuel and oxygen crossover and lower operation temperature limit their wide-spread application. Aromatic hydrocarbon polymers have been extensively studied as alternative materials for PEMs [2–7].

Sulfonated polyimides (SPIs) with six-membered imide rings have been studied as one of the promising candidates for PEMs, because of their low fuel crossover, high mechanical property and good film-forming ability [7–36]. The SPIs derived from 1,4,5,8-naphthalenetetracarboxylic dianhydride (NTDA), 2,2′-benzidinedisulfonic acid (BDSA) and different nonsulfonated diamines showed fairly good performance and durability for PEFCs at 60 °C, but the durability significantly decreased at higher temperatures above 70 °C due to the hydrolysis of imide ring [8–10]. In order to improve the water stability, the relationship of water stability and chemical structure of SPIs has been extensively investigated [7,11–28,33–36]. The water stability was a result of the total effect of hydrolysis stability, solubility stability and swelling stress stability and significantly depended on the chemical structure of sulfonated diamine [7,21,22]. The typical examples of SPIs based on the sulfonated diamines which lead to the better water stability of SPI membranes are shown in Fig. 1. The SPIs based on 4,4′-bis(4-aminophenoxy) biphenyl-3,3′-disulfonic acid (BAPBDS) maintained the high proton conductivity and fairly high tensile strength after aging in water at 130 °C for 192 h, and showed the fairly high PEFC performance and durability [7,12,30]. The SPIs based on 2,2′-bis(4-sulfophenyl) benzidine (BSPhB) showed large weight losses of more than 20% and as a result large decreases in the proton conductivity at lower relative humidities after aging in water at 130 °C for 192 h [25]. This is probably due to the too rigid structure of naphthalimide composed of NTDA and BSPhB. On the other hand, the SPIs based on 2,2′-bis(4-sulfophenoxy)benzidine (BSPOB) showed the best water stability [18,19]. They maintained the high proton conductivity and mechanical strength even after aging in water at 130 °C for 500 h, and showed the high PEFC performance and durability at 90 °C for more than 1600 h [32].

It is interesting to investigate the properties of the SPIs based on the sulfonated diamine having both the stable sulfophenyl pendant groups and the flexible ether groups. In this paper, a side-chain type diamine, 4,4′-bis(4-aminophenoxy)-3,3′-bis(4-sulfophenyl)biphenyl (BAPSPB) is synthesized and a series of BAPSPB-based SPIs are prepared and their properties are

* Corresponding author. Tel.: +81 0836 85 9660; fax: +81 0836 85 9602.
E-mail address: okamotok@yamaguchi-u.ac.jp (K.-i. Okamoto).

0032-3861/$ – see front matter © 2008 Elsevier Ltd. All rights reserved.
doi:10.1016/j.polymer.2008.11.020

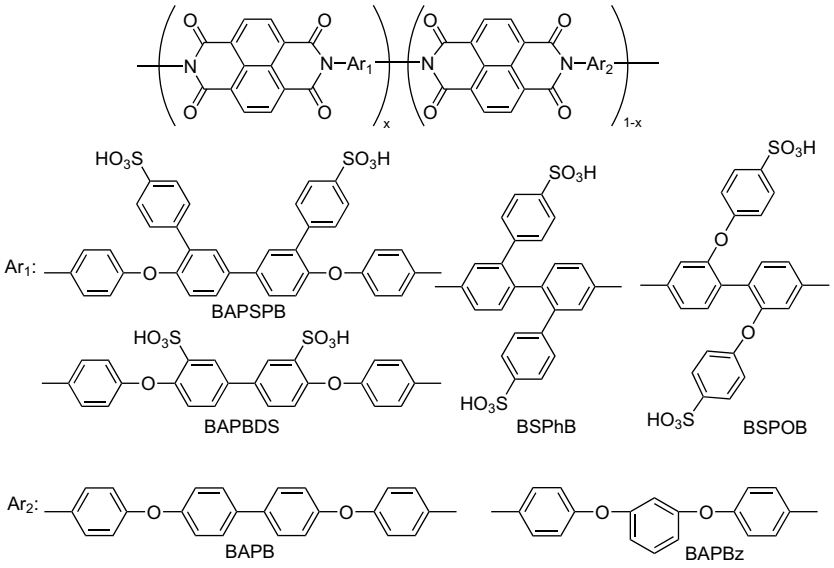

Fig. 1. Chemical structure of SPIs having better water stability of membrane.

investigated compared with the BAPBDS-, BSPhB- and BSPOB-based SPIs.

2. Experimental

2.1. Materials

Bromine, hydrobromic acid, dimethyl sulfate, 4,4′-dihydroxybiphenyl, 4,4′-bis(4-aminophenoxy) biphenyl (BAPB), 1,3-bis(4-aminophenoxy) benzene (BAPBz), benzoic acid, isoquinoline, *m*-cresol, 1,2-dichloroethane, dimethyl sulfoxide (DMSO), N,N-dimethyl acetamide (DMAc), N,N-dimethylformamide (DMF), 1-methyl-2-pyrrolidone (NMP), toluene, ethanol, methanol, isopropanol, palladium/activated carbon (Pd/C), hydrazine monohydrate, sodium hydroxide and potassium carbonate were purchased from Wako. Tetrakis(triphenylphosphine)palladium(0), phenylboronic acid and fuming sulfuric acid (60%) were purchased from Aldrich. They were used as-received. NTDA (Aldrich) was purified by vacuum sublimation before use. Triethylamine (TEA) was dried with molecular sieve of 4 Å prior to use. Ultra pure water was obtained from a Millipore Mill-Q purification system.

2.2. Synthesis of BAPSPB

Scheme 1 shows the synthesis route of the novel sulfonated diamine, BAPSPB.

2.2.1. Synthesis of 4,4′-dimethoxyl-3,3′-bis(bromo)biphenyl (DMOBB)

In a 500 ml flask, 47.9 g (300 mmol) of bromine was added dropwise into a mixture of 30.0 g (140 mmol) of 4,4′-dimethoxylbiphenyl, which was prepared from 4,4′-dihydroxybiphenyl and dimethyl sulfate, and 120 ml of acetic acid at 40 °C under stirring. The mixture was heated at 120 °C for 2 h, cooled to room temperature, and 100 ml of 30 wt% aqueous sodium hydroxide solution was added to neutralize the excess bromine. The resulting precipitate was filtered off, and washed with water to neutral. The crude product was purified by re-crystallization from ethyl acetate. Yield: 75%. ^{1}H NMR ($CDCl_3$-*d*; ppm): 6.94 (d, 2H), 7.42 (d, 2H), 7.71 (s, 2H), 3.91 (s, 3H).

2.2.2. Synthesis of 4,4′-dihydroxyl-3,3′-bis(phenyl)biphenyl (DHOPB)

To a 1000 ml flask equipped with a N_2 inlet/outlet, 9.31 g (25 mmol) of DMOBB, 7.33 g (60 mmol) of phenylboronic acid, 350 ml of toluene and 350 ml of ethanol were charged. The solid was completely dissolved at 50 °C under stirring. 150 ml of 10 wt% aqueous sodium carbonate solution and 0.58 g (0.50 mmol) of tetrakis(triphenylphosphine)palladium(0) were carefully added into the solution. The reaction mixture was heated at 80 °C for 20 h, and then the solvent was evaporated to obtain the solid. The resulting solid was dissolved in 1,2-dichloroethylane/water system and the catalysts were eliminated by filtration. The organic phase was washed with water to neutral. The solid was obtained by evaporating the solvent and purified by re-crystallization from toluene/ethanol system. 4,4′-Dimethoxyl-3,3′-bis(phenyl)biphenyl thus prepared was reacted with aqueous HBr solution to obtain DHOPB. Yield: 76%. ^{1}H NMR ($CDCl_3$-*d*; ppm): 7.04 (d, 2H), 7.33 (d, 2H), 7.40 (d, 2H), 7.45 (d 4H), 7.54 (d, 4H), 7.57 (s, 2H).

2.2.3. Synthesis of 4,4′-bis(4-nitrophenoxy)-3,3′-bis(phenyl)-biphenyl (BNPPB)

To a 200 ml completely dried flask, equipped with N_2 inlet and outlet, 6.77 g (20 mmol) of DHOPB, 5.64 g (40 mmol) of 4-fluoro-1-nitrobenzene, 5.53 g (40 mmol) of potassium carbonate and 88 ml of DMF were charged and stirred at room temperature for 1 h. The reaction solution was heated at 80 °C for 20 h. The solvent was distilled away under vacuum to obtain the solid. The crude product was obtained by washing with water to neutral, and purified by re-crystallization from ethyl acetate. Yield: 80%. ^{1}H NMR ($CDCl_3$-*d*; ppm): 6.93 (dd, 4H), 7.22 (d, 2H), 7.31 (d, 2H), 7.36 (d, 2H), 7.48 (d, 4H), 7.68 (dd, 4H), 7.76 (s, 2H), 8.12 (d, 4H).

2.2.4. Synthesis of 4,4′-bis(4-nitrophenoxy)-3,3′-bis-(4-sufophenyl)biphenyl (BNPSPB)

To a 100 ml flask, 17.42 g (30 mmol) of BNPPB and 43.2 ml of concentrated sulfuric acid were charged, stirred for 1 h, and then 4.8 ml of fuming sulfuric acid (SO_3, 60%) was added dropwise into the mixture. The mixture was slowly heated to 40 °C and kept for 8 h. After cooled to room temperature, the solution was poured into 300 ml ice water. To the solution, 70 g sodium chloride was added. The solid was filtered off and washed with water to neutral. Yield: 80%. ^{1}H NMR (DMSO-d_6; ppm): 7.08 (d, 4H), 7.37 (d, 2H), 7.56 (d, 2H), 7.64 (d 4H), 7.91 (s, 2H), 7.97 (d, 4H), 8.18 (d, 4H).

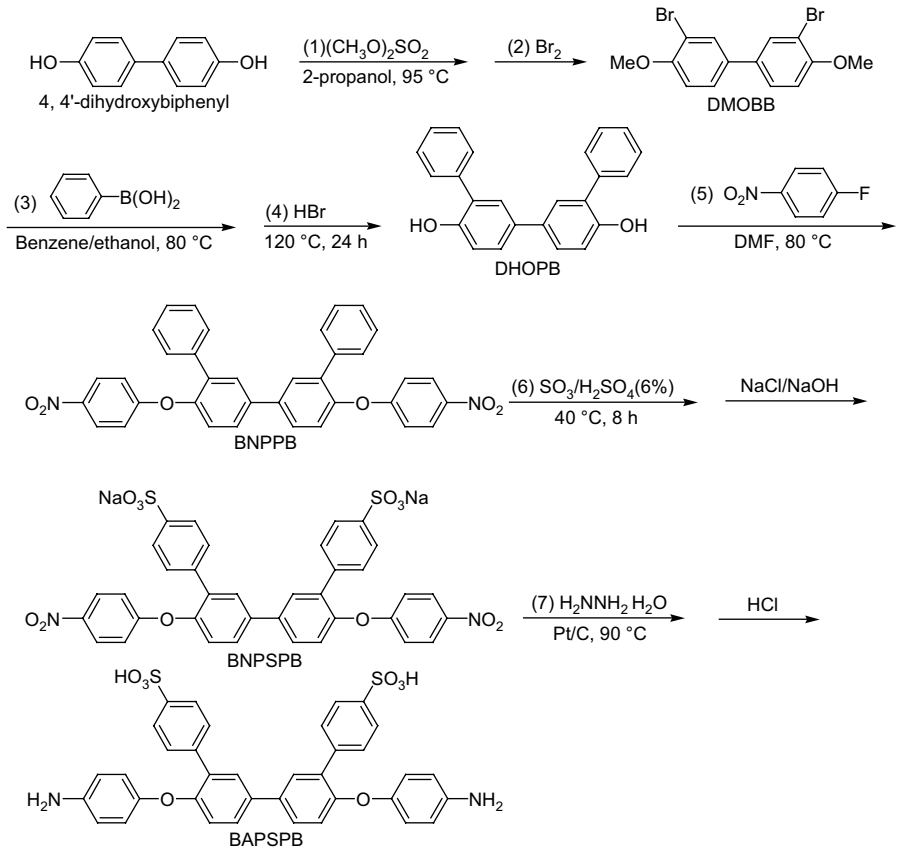

Scheme 1. Synthesis of BAPSPB.

2.2.5. Synthesis of 4,4′-bis(4-aminophenoxy)-3,3′-bis(4-sulfophenyl)biphenyl (BAPSPB)

To a 500 ml flask equipped with N_2 inlet and outlet, 7.41 g (10 mmol) of BNPSPB, 250 ml of water and 0.4 g of Pd/C were charged. The solution was heated to 90 °C and 8 ml of hydrazine monohydrate was added dropwise. The reaction mixture was stirred at 90 °C for 20 h, and then cooled to room temperature. The catalyst Pd/C was filtered off. 100 ml of concentrated HCl was added to the filtrate under nitrogen atmosphere to get the precipitate. The pale precipitate was filtered and washed with water to neutral. The crude product was purified by re-crystallization from water. Yield: 85%. Elemental analysis result: Calculated for $C_{36}H_{28}N_2O_8S_2$: C, 63.52%; H, 4.15%; N, 4.12%. Calculated for containing 8.0% water in the sample: C, 58.41%; H, 4.71%; N, 3.78%. Found: C, 56.80%; H, 4.60%; N, 3.70%.

2.3. Synthesis of BAPSPB-based sulfonated polyimides

A series of homo- and co-SPIs derived from NTDA, BAPSPB and BAPB or BAPBz were synthesized. As an example, the synthesis of NTDA–BAPSPB/BAPB (3/1) is described below, where the data in the parenthesis refer to the molar ratio of BAPSPB to BAPB.

To a 200 ml completely dried flask equipped with N_2 inlet and outlet, 4.085 g (6.00 mmol) of BAPSPB, 38 ml of *m*-cresol and 2.04 ml of TEA were added successively. After BAPSPB was completely dissolved, 0.737 g of (2.00 mmol) BAPB, 2.145 g (8.00 mmol) of NTDA and 2.32 g of benzoic acid were added. The mixture was heated at 80 °C for 4 h and 180 °C for 12 h, and then 2.06 g of isoquinoline was added to the flask, the reaction was continued at 180 °C for another 12 h. After cooling to 80 °C, 60 ml of *m*-cresol was added to dilute the highly viscous solution, and then precipitated into acetone. The fiber-like precipitate was washed with acetone, extracted with 2-propanol and dried in vacuum at 60 °C for 5 h. Elemental analysis result: Calculated for NTDA–BAPSPB/BAPB (3/1) in H^+ form ($C_{189}H_{111}N_8O_{42}S_6$) C, 67.59%; H, 3.33%; N, 3.34%. Calculated for containing 7.9% water in the sample: C, 62.25%; H, 3.95%; N, 3.07%. Found: C, 57.60%; H, 3.90%; N, 3.10%.

2.4. Membrane formation and proton exchange

SPI membranes were prepared by casting from *m*-cresol solution (5–7 wt%) onto glass plates and drying at 80 °C for 2 h and then at 120 °C for 12 h. The as-cast membranes were soaked in methanol for 24 h to remove the residual solvent, and then treated with 1.0 N HCl solution at 50 °C for 72 h for proton exchange. The proton-exchanged membranes were soaked in water at room temperature for 48 h and cured in vacuum at 150 °C for 1 h and 180 °C for 1 h.

2.5. Measurements

^{1}H NMR spectra were recorded on a JEOL EX270 (270 MHz) instrument. FTIR spectra were recorded on a Horiba FT-200 Spectrometer as polymer membranes. The reduced viscosity η_r was measured with an Ostwald viscometer with 0.5 g/dl *m*-cresol solution at 35 °C. Thermogravimetric analysis (TGA) was performed on Rigaku TG-8120 in helium (flow rate: 100 cm^3/min) at a heating rate of 10 °C/min. Mechanical tensile tests were performed on a universal testing machine (Orientic, TENSILON TRC-1150A) at 25 °C and about 60% RH.

Water vapor sorption isotherms were measured at 60 °C and water vapor activities a_w less than 0.93 using a sorption apparatus (BEL-18SP) by means of a volumetric method. The weight of

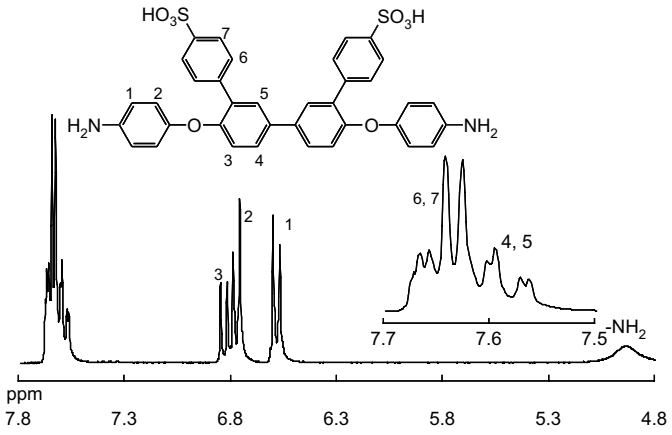

Fig. 2. ^{1}H NMR spectrum of BAPSPB in DMSO-d_6.

membrane sample used was 80–100 mg. Water uptake (WU) was measured by immersing an SPI membrane sample into water at 60 °C for 24 h. Then the membrane was taken out, wiped with tissue paper very quickly, and weighed on a microbalance. Water uptake was calculated from:

$$\mathrm{WU} = (W_s - W_d)/W_d \times 100\%$$

where W_d and W_s are the weights of dry and corresponding water-swollen membranes, respectively.

Dimensional change in membrane thickness (Δt_c) and diameter (Δl_c) were measured by immersing more than two samples in water at 30 °C for 5 h. The changes of thickness and diameter were calculated from:

$$\Delta t_c = (t - t_s)/t_s$$

$$\Delta l_c = (l - l_s)/l_s$$

where t_s and l_s are the thickness and diameter of the membrane equilibrated at 70% RH, respectively; t and l refer to those of the membrane immersed in liquid water.

Ion exchange capacity (IEC) of membrane was determined by the titration method. A sample membrane in proton form was soaked in a 15 wt% NaCl solution for 72 h at 40 °C to exchange the H^+ ion with Na^+ ion. Released protons were titrated by 0.02 N NaOH solution using phenolphthalein as an indicator.

Proton conductivity in plane direction of membrane was determined using an electrochemical impedance spectroscopy technique over the frequency from 10 Hz to 100 kHz (Hioki 3532-80). A single cell with two platinum plate electrodes was mounted on a Teflon plate at 0.5 cm distance. The cell was placed under either in a thermo-controlled humidic chamber or in liquid water. Proton conductivity, σ, was calculated from:

$$\sigma = d/(t_s w_s R)$$

where d is the distance between the two electrodes, t_s and w_s are the thickness and width of the membrane at a standard condition of 70% RH, respectively, and R is the resistance value measured. For the measurements in liquid water, the swollen membrane thickness was used in the calculation of σ.

Water stability tests were carried out by immersing SPI membrane sheets (150–200 mg of dry weight, in proton form) into ultra pure water (90 ml) at 130 °C in an autoclave, which was set in the thermo-controlled oven, for a given time (48–500 h).

Membrane electrode assembly (MEA) was fabricated by sandwiching an SPI membrane with two gas diffusion electrodes using 5 wt% Nafion solution as a binder. The anode and cathode electrodes were purchased from Johnson Matthey (45372). The MEA was hot-pressed at 150 °C for 5 min under 60 kg/cm^2. The MEA was positioned into a single-cell test fixture (NF Inc., active area: 5 cm^2) and mounted into an in-house fuel cell test station (NF Inc., model As-510), which was supplied with temperature-controlled humidified gases. The PEFC performance was evaluated at a cell temperature of 90 °C, a gas pressure of 0.3 MPa and a gas humidifier temperature of 72 °C corresponding to 50% RH.

3. Results and discussion

3.1. Monomer synthesis

As shown in Scheme 1, BAPSPB was synthesized by seven steps of reactions with an overall yield of 32%. BNPSPB was synthesized by direct sulfonation of BNPPB. BNPPB was dissolved in concentrated sulfuric acid at room temperature, and sulfonated with fuming sulfuric acid (6% SO_3) at 40 °C for 8 h. Under this condition the sulfonation took place only on the more electron-rich positions, namely 4- and 4′-positions of the pendant phenyl rings because these two positions are more reactive than the other ones. The chemical structure of BAPSPB was characterized by ^{1}H NMR spectrum as shown in Fig. 2. All peaks were well assigned to each proton and the integration intensity ratio of the protons was in agreement with the theoretical data. The elementary analysis results were slightly different from the calculated ones. This was attributed to a small amount of sorbed water (8.0%) in the sample.

Table 1
Physical properties of NTDA-based SPIs.

Code	NTDA-based SPIs	IEC[a] (mequiv/g)	η_r[b] (dl/g)	WU[c] (%)	λ	Dimensional change[d]		σ (mS/cm)[c]		
						Δt_c	Δl_c	50% RH	70% RH	In water
M1	BAPSPB	2.19(2.08)	6.4	68	17	0.23	0.097	8.3	34	135
M2	BAPSPB/BAPB(3/1)	1.80(1.69)	4.1	49	15	0.14	0.054	7.2	26	104
M3	BAPSPB/BAPB(2/1)	1.65(1.50)	6.9	43	14	0.11	0.027	3.0	13	56
M4	BAPSPB/BAPBz(3/1)	1.84(1.72)	6.2	50	15	0.15	0.063	6.3	24	103
M5	BAPSPB/BAPBz(2/1)	1.70(1.50)	10.5	45	15	0.16	0.051	4.4	20	85
R1	BAPBDS/BAPB(2/1)	1.89(1.86)	4.9	57[d]	17	0.14	0.049	5.4	29	127
R2	BAPBDS/BAPBz(2/1)	1.96	2.0	55[d]	16	0.14	0.070	2.3	13	102
R3	BSPOB/BAPB(2/1)	1.89(1.94)	3.9	78[d]	23	0.39	0.026	7.0	30	168
R4	BSPhB/BAPB(3/2)	1.77(1.58)	6.0	60[d]	19	0.34	0.030	8.0	27	121

[a] Calculated data, data in parentheses were obtained by titration.
[b] 0.5 g dl^{-1} in *m*-cresol at 35 °C.
[c] At 60 °C.
[d] At 30 °C.

3.2. Polymer synthesis and characterization

Preparation of BAPSPB-based homo- and co-SPIs was carried out through the one-pot high temperature polymerization method in *m*-cresol in the presence of TEA, benzoic acid, and isoquinoline. The addition of isoquinoline was reported to have positive effects on the imidization and molecular weight [37]. The elemental analysis of polymer showed differences between the calculated and found data due to the sorbed water in the sample. After correction of water content of 7.9% in the sample, the calculated and found data were in agreement. Table 1 lists the physical properties of the BAPSPB-based SPI membranes (Code No. M1–M5). For comparison, the data for the BAPBDS- and BSPOB- and BSPhB-based SPIs (R1–R2, R3 and R4, respectively) are also listed. The viscosity values of the BAPSPB-based SPIs were higher than 4 dl/g, indicating the high molecular weight. Tough, flexible and transparent membranes of 30–45 μm in thickness were obtained. The IEC values determined by the titration method were a little smaller than the calculated ones.

Fig. 3 shows the IR spectra of BAPSPB-based SPI membranes in proton form. The spectra displayed the absorption bands of naphthalene imide rings at 1712 (C═O symmetric), 1666 (C═O asymmetric) and 1350 cm^{-1} (C–N asymmetric). The stretch vibration (O═S═O) of sulfonic acid group was detected at 1200, 1100 and 1030 cm^{-1}. The characteristic peak of polyamic acid at 1780 cm^{-1} was not detected, indicating the complete imidization.

The BAPSPB-based SPIs in TEA salt form were soluble only in *m*-cresol but not in proton form. They were insoluble in DMSO, NMP and DMAc in both forms. This solubility behavior was similar to that of the BAPBDS-based SPIs and slightly different from that of the BSPOB-based ones.

3.3. Thermal and mechanical properties

The thermal stability of SPIs in proton form was investigated by TGA. Above 150 °C, the two-step degradation profile was observed for all of the SPIs. The weight loss below 400 °C was attributed to the cleavage of sulfonic acid group, whereas the weight loss above 500 °C was attributed to the decomposition of polymer backbone. The first decomposition (desulfonation) temperature (T_{d1}) was 325 °C for the BAPSPB-based SPIs, which was similar to that for the BSPhB-based SPIs and higher than that (300–310 °C) for the BAPBDS- and BSPOB-based SPIs, indicating the improved thermal stability of the sulfonic acid group for the BAPSPB- and BSPhB-based SPIs than for the BAPBDS- and BSPOB-based ones.

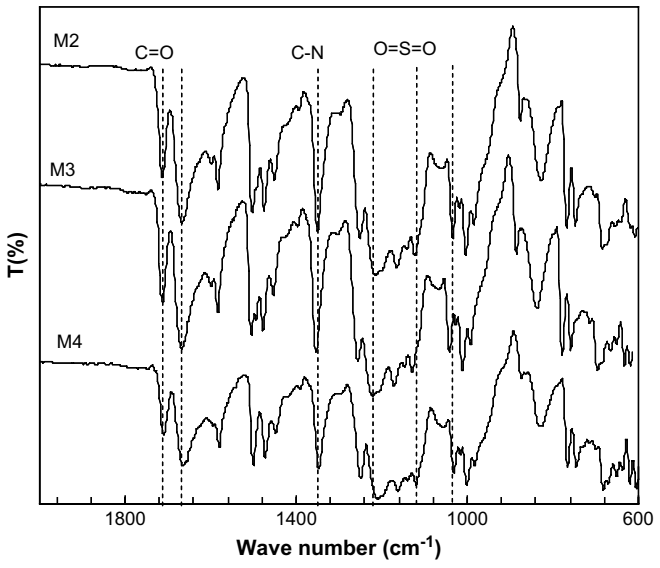

Fig. 3. FTIR spectra of BAPSPB-based SPI membranes in proton form.

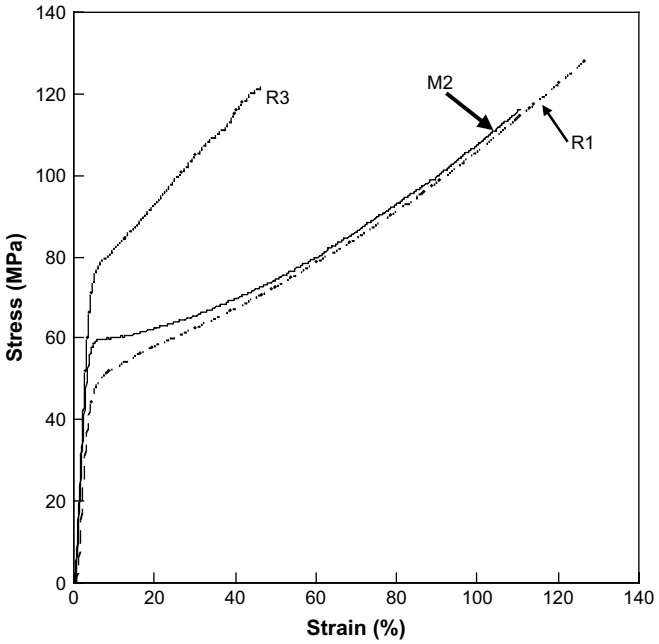

Fig. 4. Tensile stress–strain curves of SPI membranes.

Fig. 4 shows the tensile stress–strain curves of SPI membranes. The mechanical property was characterized by Young's modulus *M*, maximum stress *S* and elongation at break *E*. The data are listed in Table 2. The tensile strength behavior of the BAPSPB-based SPIs was similar to that of the BAPBDS-based one (R1) and different from that of the BSPOB-based one (R3). The latter had a higher Young's modulus and yield point, but lower elongation after the yield point to the break point, and as a result the maximum stress was similar to the formers. This indicates that the BSPOB-based SPI membranes were slightly stiffer than the BAPSPB- and BAPBDS-based ones.

Table 2
Properties of the SPI membranes before and after aging in water at 130 °C.

Code	Time[a] (h)	IEC[b] (mequiv/g)	WL[c] (%)	*M*[d] (GPa)	*S*[e] (MPa)	*E*[f] (%)	σ (mS/cm) [g]		
							50%	70% RH	In water
M2	0	1.69		1.8	109	116	7.2	26	104
	48		5	1.6	54	9	7.8	26	95
	192		7	1.1	45	7	4.4	24	98
	500	1.42	15	1.3	42	6	5.3	26	99
M3	0	1.56		1.8	106	116	3	13	56
	500	1.36	15	1.6	55	8	2.4	11	52
R2	0	1.86		1.4	81	95	2.3	13	102
	192		7	1.2	55	10	2.9	13	103
R3	0	1.84		2.9	122	45	7	30	168
	192		10	2	76	8	6.2	31	166
	500	1.66	15	1.9	67	6	5	27	160
R4	0	1.58		1.3	99	103	8	27	121
	192		25	1.3	36	5	2	13	97

[a] Soaking time.
[b] By titration.
[c] Weight loss.
[d] Young's modulus.
[e] Stress at break.
[f] Elongation at break.
[g] At 60 °C.

3.4. Water vapor sorption, water uptake and dimensional change

The water vapor sorption and water uptake in water mainly depend on the IEC of membrane, and the comparison of them among the membranes with different IECs is often performed in terms of the number of water molecules sorbed per sulfonic acid group, λ. In this study, the λ values were calculated using the theoretical IEC values (calculated from molar ratio in feed). Water vapor sorption isotherms of BAPSPB-based SPIs (M1, M2) at 60 °C are shown as the plots of λ versus water vapor activity a_w in Fig. 5, together with those of the BAPBDS- and BSPOB-based SPIs (R1, R3) for comparison. With an increase in a_w, the water vapor sorption increased sigmoidally. This was explained by means of the dual-mode (Langmuir type and Henry type) sorption and the plasticization effect of sorbed water at the high activities above 0.7 [38]. At the activities below 0.7, the sorption isotherms of BAPSPB- and BSPOB-based SPIs (M1, M2 and R3) were similar to each other and their λ values were slightly smaller than those of the BAPBDS-based SPI. With an increase in a_w from 0.7, the λ increased largely for R1 and R3, but not so for M1 and M2, indicating the smaller plasticization effect of sorbed water for the BAPSPB-based SPI membranes than for the BAPBDS- and BSPOB-based ones. This reflected the behavior of water uptake in water.

In water, the BAPSPB-based SPIs showed the similar λ values of 14–17, which were comparable to that (16–17) of BAPBDS-based SPIs and smaller than those (19–23) of BSPOB- and BSPhB-based SPI membranes. These SPIs displayed anisotropic membrane swelling with larger dimensional change in thickness direction than in plane, as summarized in Table 1. The anisotropic degree of membrane swelling was defined as $\Delta t_c/\Delta l_c$ in this study. The anisotropic degree was 2.5–4 for the BAPSPB-based SPIs, which was comparable to that for the BAPBDS-based SPIs and much smaller that that (about 10) for the BSPOB- and BSPhB-based ones. The anisotropic membrane swelling of SPI membranes is considered due to the polymer chain alignment in plane direction. The rigid imide backbone from NTDA and benzidine with sulfonated pendants seems to cause the better alignment of polymer chain in plane direction compared with the imide backbone containing flexible ether bonds. As mentioned above, the BAPSPB-based SPIs showed the similar membrane swelling behavior to BAPBDS-based SPIs.

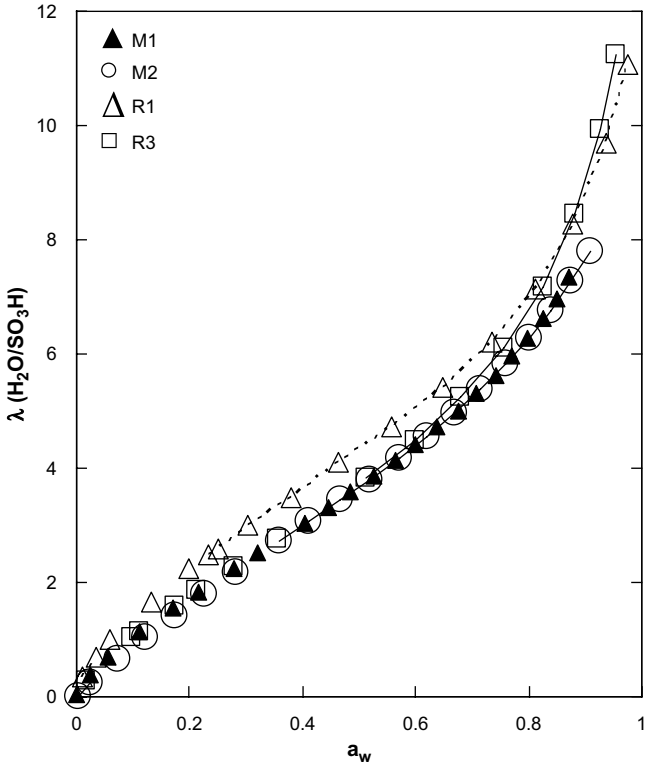

Fig. 5. Water vapor sorption isotherms of SPIs at 60 °C.

3.5. Proton conductivity

Fig. 6 shows the relative humidity dependence of proton conductivity at 60 °C. Table 1 also lists the conductivity values at 50 and 70% RH and in water at 60 °C. The SPI membranes generally displayed larger RH dependence of conductivity than Nafion 112. For example, the σ value in water was almost the same for M1 and Nafion, whereas the σ value at 50% RH was 3.6 times larger for Nafion. In comparison of the conductivity among the SPIs (M2, R1 and R3) with the similar IEC values of 1.80–1.89 mequiv/g, the σ value in water was in the order of R3 > R1 > M2. This was attributed to the difference in λ. On the other hand, the σ value at lower RH (50% RH) was in the order of R3 = M2 > R1.

The proton conductivity significantly depends on the water content sorbed in membrane. Fig. 7 shows the plots of log conductivity versus inverse of water content C_w for the SPIs and Nafion 112. In the upper and left region in the figure referring to the highly hydrated state, the membranes with the similar water content had the similar conductivity irrespective of their polymer structures. With decreasing water content, the conductivity decreased largely. There was roughly observed a linear relationship between log σ and C_w^{-1} for each type of membrane, as shown in Fig. 7. The relation line of M2 was very close to that of R3 and far from that of R1. In comparison at a lower water content, the conductivity was in the order of Nafion ≫ M2 = R3 > R1. The BAPSPB- and BSPOB-based SPI membranes showed the better conductivity performance in the lower water content range than the BAPBDS-based SPI membranes. This might be due to some difference in membrane morphology, although TEM observation indicated the similar homogeneous structure without any contrast for these SPI membranes.

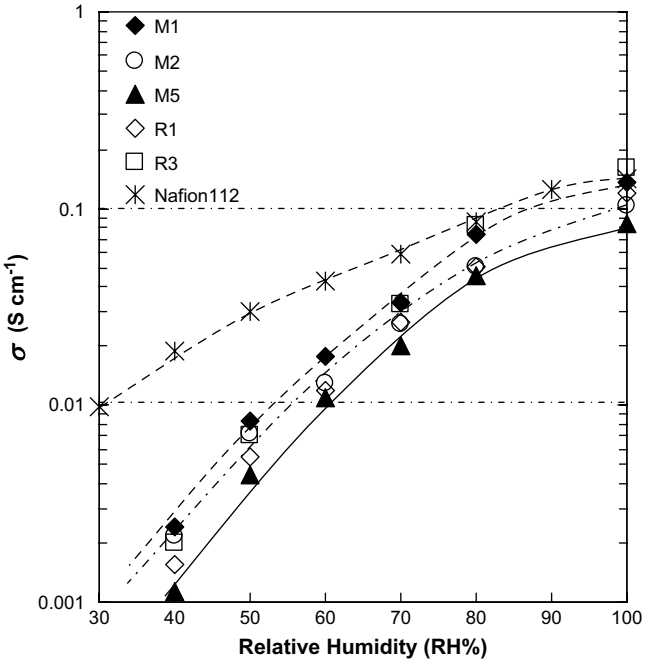

Fig. 6. Relative humidity dependence of proton conductivity of SPI membranes and Nafion 112 at 60 °C.

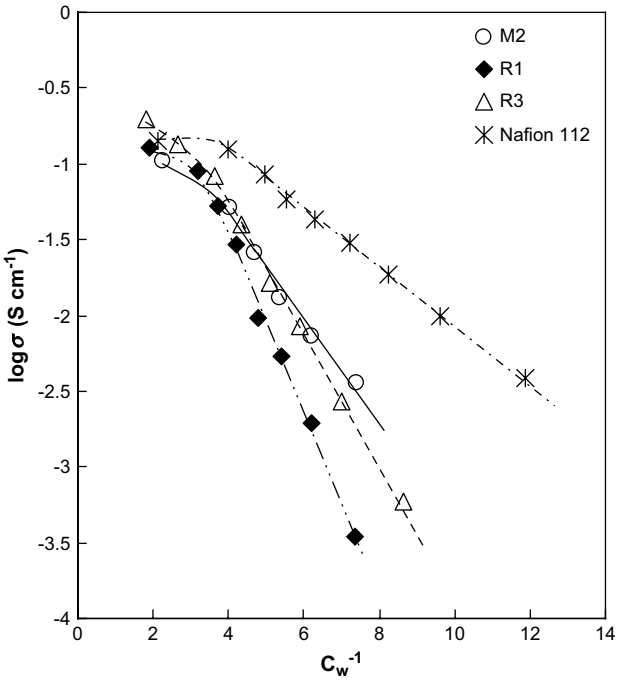

Fig. 7. Plots of log σ versus C_w^{-1} for SPI membranes and Nafion 112 at 60 °C.

Fig. 8 shows the temperature dependence of proton conductivity for SPI membranes in water. The activation energy of conductivity for the BAPSPB-based SPIs was in range of 11–13 kJ/mol, which was similar to that (12 kJ/mol) for R1 and R3.

3.6. Water stability

The water stability of SPI membranes was evaluated by means of an accelerated hydrolytic stability test. The membranes were soaked in pressurized water at 130 °C for 48–500 h, followed by the investigation of weight loss, proton conductivity and mechanical properties.

Fig. 9 shows the FTIR spectra of M2 before and after aging in water at 130 °C for 500 h. There was observed no appreciable change except the appearance of very weak peaks of acid anhydride carbonyl at 1785 and 1750 cm^{-1} after aging. However, the acid anhydride carbonyl peaks were much smaller than the imide carbonyl peak at 1712 cm^{-1}. It is noted that the dicarboxylic acid of the model compound, N-(3-sulfophenyl)-4,5-dicarboxylic-1,8-naphthalimide, was easily converted to the acid anhydride by drying it under vacuum at 100 °C. Therefore, these results indicate that the hydrolysis of the imide ring to carboxylic acid and amine took place to some extent in the aging, resulting in a reduction in the molecular weight.

Table 2 lists the weight loss (WL), proton conductivity and mechanical property of the SPI membranes before and after the aging tests. For comparison, the data of the other SPI membranes, R1, R3 and R4, are also listed [19,22,25]. The reduction of molecular weight was reflected in the change in tensile strength property with the aging. The aged membrane displayed much smaller elongation after a yield point until a break point, compared to the unaged one. As a result, the aged sample displayed smaller maximum stress and much smaller elongation at break than the unaged one, although Young's modulus was not so different between them. Such a change in the tensile strength property took place in the initial period (48 h) of the soaking and the further soaking until 500 h slightly reduced the tensile strength property. As a result, after soaking for 500 h, M2 and M3 still kept reasonably high Young's modulus and maximum stress of 1.3–1.6 GPa and 42–55 MPa, respectively, but relatively small elongation at break of 6–8%. After aging for 500 h, the BAPSPB-based SPI membranes also showed good membrane toughness in the bending test, that is, the membrane sheet did not break after it was folded and then folded back [12,22].

The BAPSPB-based SPI membranes M2 and M3 showed the weight loss of 15% after aging for 500 h, which were the same as that for the BSPOB-based SPI membrane R3. The FTIR spectrum was measured for the residue on distillation of soaking water solution for M2 and is also shown in Fig. 9. Compared with the aged membrane, the residue showed much larger anhydride carbonyl

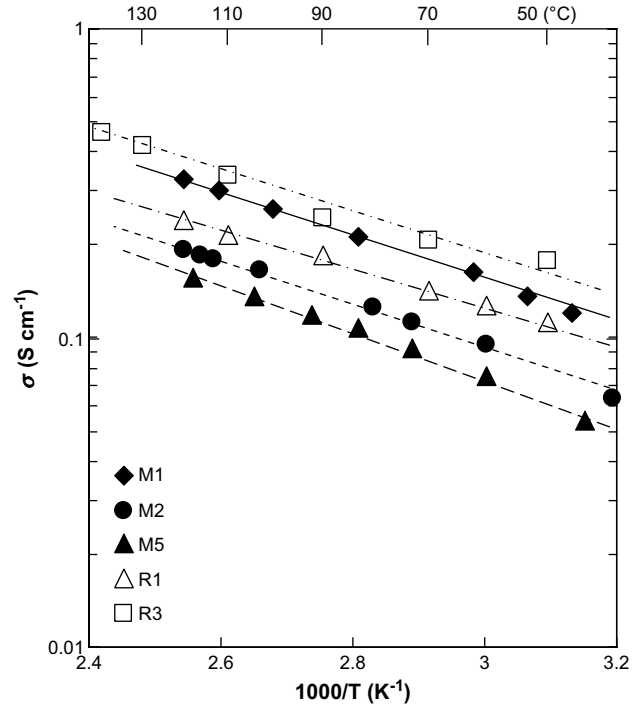

Fig. 8. Temperature dependence of proton conductivity of SPI membranes in water.

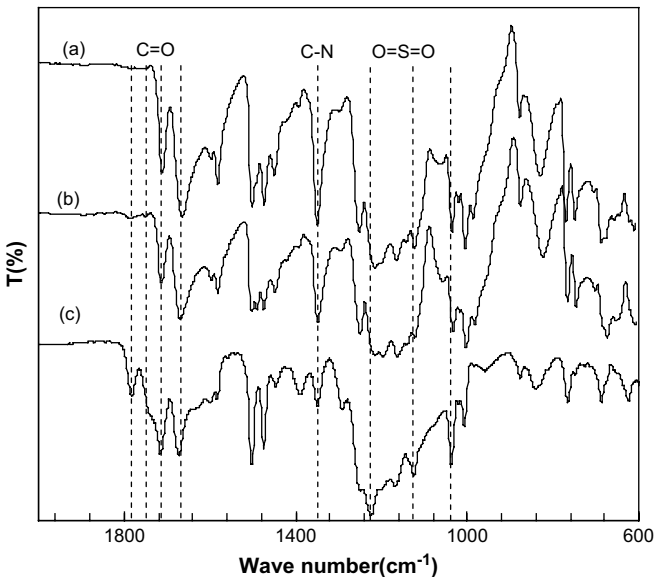

Fig. 9. FTIR spectra of M2 (a) before aging; (b) after aging and (c) the residue on distillation of soaking water solution.

peaks, much smaller imide carbonyl and C–N peaks and larger sulfonic acid O═S═O peaks. This suggests that the hydrophilic naphthalimide oligomer with carboxylic acid terminal groups formed by the hydrolysis dissolved into the soaking water solution. After aging for 500 h, the IEC values measured by the titration for M2 and M3 decreased from the original ones of 1.69 and 1.56 mequiv/g, respectively down to 1.42 and 1.36 mequiv/g. The reductions in IEC were 16 and 13%, respectively, which were comparable to the weight losses.

As listed in Table 2, the conductivity at 50, 70% RH and in water for M2 and M3 was hardly reduced after aging, in spite of the fairly large weight loss and IEC reduction. This was similar to the case of R1 and R3, whereas R4 showed the large decrease in the conductivity especially at the lower relative humidities because of the large weight loss of 25%. This suggests that the hydrolysis of polymer chain took place mainly in the more hydrophilic part, followed by the dissolution of the hydrophilic oligomer, but the remained part still kept the hydrophilic level enough to conduct protons in the former case. The proton conductivity was mainly controlled by the less hydrophilic part.

As mentioned above, the BAPSPB-based SPI membranes displayed high proton conductivity, high membrane toughness and high tensile strength even after aging in water at 130 °C for 500 h. It was found in this study that the BAPSPB-based SPIs had high water stability of membrane, which was comparable to that for the BSPOB-based SPIs and much better than that for the other SPIs derived from BAPBDS, BSPhB and other sulfonated diamines reported so far [9–17,21–25].

3.7. Fuel cell performance

Fig. 10 shows the PEFC performances for M4, R3 and Nafion 112 with supply of air into the cathode. The gas flow rates were controlled to keep constant utilization of H_2 at 70% and of O_2 in air at 32% at a humidification temperature of 72 °C, although the lowest gas flow rate was limited at 30 Ncm^3/min. The polarization curves for these three membranes almost overlapped up to the load current density of 1.3 A/cm^2. In the range of high current density above 1.3 A/cm^2, there were observed differences in the polarization curves among them due to the different magnitude of the mass transfer resistance. The BAPSPB-based SPI membrane (M4) showed the high PEFC performance, for example, open circuit voltage (OCV) of 0.97 V, cell voltage at current density of 1 A/cm^2 (V_1) of 0.64 V and maximum output (W_{max}) of 0.79 W/cm^2, which were comparable to those for the BSPOB-based SPI (1.00 V, 0.65 V, and 0.86 W/cm^2, respectively) and for Nafion 112 (0.93 V, 0.64 V and 0.79 W/cm^2, respectively). Even under a low humidification of 50% RH, these SPI membranes displayed high PEFC performances. This was attributed to the enhanced water content in membrane due to the back diffusion of water formed at the cathode.

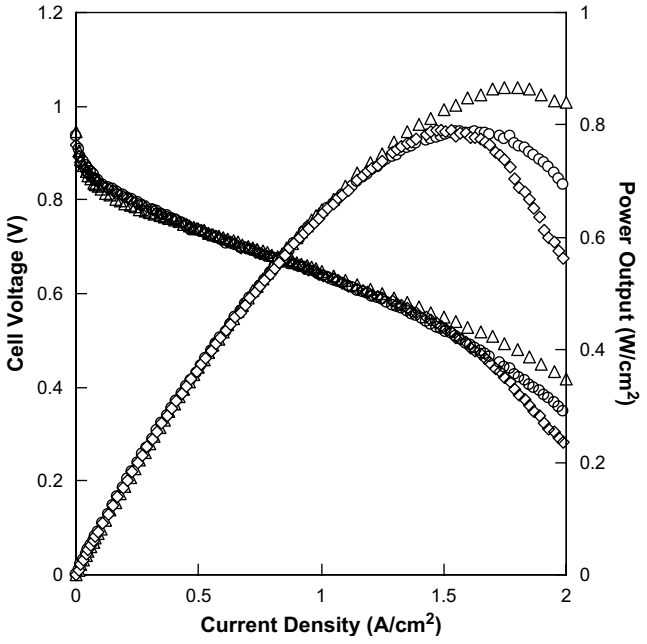

Fig. 10. PEFC performance for SPI membranes and Nafion 112 at 90 °C and 0.3 MPa. (○: M4, △: R3, ◇: Nafion 112.)

The PEFC operation experiments were continued for about 300 h and there was observed no reduction in the cell performance, indicating the short term durability of PEFCs with BAPSPB-based SPI membranes. The long term durability test and more detailed PEFC performance were under investigation.

4. Conclusions

The BAPSPB-based SPI membranes showed anisotropic membrane swelling in water with 2.5–4 times larger dimensional change in thickness direction than in plane. The anisotropy was comparable to that for the BAPBDS-based SPIs and much smaller than that for the BSPOB- and BSPhB-based SPIs. There was roughly observed a linear relationship between log σ and C_w^{-1} for each type of membrane. The BAPSPB-based SPI membranes showed the high conductivity performance in the lower water content range, which was comparable to that of the BSPOB-based ones and better than that of the BAPBDS-based ones. The BAPSPB-based SPI membranes maintained high mechanical strength and conductivity after aging in water at 130 °C for 500 h, showing their high water stability comparable to that of the BSPOB-based ones and better than that of the BAPBDS-based ones. In a single cell system at 90 °C, they showed high cell performances under a low humidity of 50% RH due to the back diffusion of water formed in the cathode, which were comparable to those of the BSPOB-based SPI membranes and Nafion 112. They have high potential for PEFC applications.

Acknowledgement

This work was financially supported by the New Energy and Industrial Technology Development Organization (NEDO) and by a Grand-in-aid for Development Science Research (No. 19550209) from the Ministry of Education, Science, and Culture of Japan.

References

[1] Mauritz K, Moore R. Chem Rev 2004;104:4535–85.
[2] Savadoga O. J New Mater Electrochem Syst 1998;1:47–66.
[3] Rikukawa M, Sanui K. Prog Polym Sci 2000;25:1463–502.
[4] Li Q, He R, Jensen J, Bjerrum N. Chem Mater 2003;15:4896–915.
[5] Hickner M, Ghassemi H, Kim Y, Einsla B, McGrath J. Chem Rev 2004;104:4587–612.
[6] Ghassemi H, McGrath J, Zawodzinski Jr T. Polymer 2006;47:4132–9.
[7] Yin Y, Yamada O, Tanaka K, Okamoto K. Polym J 2006;38:197–219.
[8] Cornet N, Diat O, Gebel G, Jousse F, Marsacq D, Merciere R, et al. J New Mater Electrochem Syst 2000;3:33–42.
[9] Genies C, Mercier R, Sillion B, Cornet N, Gebel G, Pineri M. Polymer 2001;42:359–73.
[10] Meyer G, Perrot C, Gebel G, Gonon L, Morlat S, Gardette J. Polymer 2006;47:5003–11.
[11] Guo X, Fang J, Watari T, Tanaka K, Kita H, Okamoto K. Macromolecules 2002;35:6707–13 and 9022–8.
[12] Watari T, Fang J, Tanaka K, Kita H, Okamoto K, Hirano T. J Membr Sci 2004;230:111–20.
[13] Yin Y, Fang J, Watari T, Tanaka K, Kita H, Okamoto K. J Mater Chem 2004;14:1062–70.
[14] Yin Y, Yamada O, Suto Y, Mishima T, Tanaka K, Kita H, et al. J Polym Sci Part A Polym Chem 2005;43:1545–53.

[15] Einsla B, Kim Y, Hickner M, Hong Y, Hill M, Pivovar B, et al. J Membr Sci 2005;255:141–8.
[16] Yasuda T, Miyatake K, Hirai M, Nanasawa M, Watanabe M. J Polym Sci Part A Polym Chem 2005;43:4439–45.
[17] Yasuda T, Li Y, Miyatake K, Hirai M, Nanasawa M, Watanabe M. J Polym Sci Part A Polym Chem 2006;44:3995–4005.
[18] Fang J, Guo X, Litt M. Trans Mater Res Soc Jpn 2004;29:2541–6.
[19] Suto Y, Yin Y, Kita H, Okamoto K. J Photopolym Sci Technol 2006;19:273–4.
[20] Yin Y, Yamada O, Hayashi S, Tanaka K, Kita H, Okamoto K. J Polym Sci Part A Polym Chem 2006;44:3751–62.
[21] Yin Y, Chen S, Guo X, Fang J, Tanaka K, Kita H, et al. High Perform Polym 2006;18:617–35.
[22] Yin Y, Suto Y, Sakabe T, Chen S, Hayashi S, Mishima T, et al. Macromolecules 2006;39:1189–98.
[23] Hu Z, Yin Y, Chen S, Yamada O, Tanaka K, Kita H, et al. J Polym Sci Part A Polym Chem 2006;44:2862–72.
[24] Chen S, Yin Y, Kita H, Okamoto K. J Polym Sci Part A Polym Chem 2007;45:2797–811.
[25] Hu Z, Yin Y, Kita H, Okamoto K, Suto Y, Wang H, et al. Polymer 2007;48:1962–71.
[26] Fang J, Zhai F, Guo X, Xu H, Okamoto K. J Mater Chem 2007;17:1102–8.
[27] Yan J, Liu C, Wang Z, Xing W, Ding M. Polymer 2007;48:6210–4.
[28] Li N, Cui Z, Zhang S, Xing W. J Membr Sci 2007;295:148–58.
[29] Alvarez-Gallego Y, Nunes S, Lozano A, de la Campa J, de Abajo J. Macromol Rapid Commun 2007;28:616–22.
[30] Yamada O, Yin Y, Tanaka K, Kita H, Okamoto K. Electrochim Acta 2005;50:2655–9.
[31] Asano N, Aoki M, Suzuki S, Miyatake K, Uchida H, Watanabe M. J Am Chem Soc 2006;128:1762–70.
[32] Okamoto K, Matsuda K, Hu Z, Chen K, Endo N, Higa M. ECS Trans 2008;12(1):5–12.
[33] Lee C, Park C, Lee Y. J Membr Sci 2008;313:199–206.
[34] Miyatake K, Yasuda T, Watanabe M. J Polym Sci Part A Polym Chem 2008;46:4469–78.
[35] Bai H, Ho W. J Membr Sci 2008;313:75–85.
[36] Chen X, Yin Y, Chen P, Kita H, Okamoto K. J Membr Sci 2008;313:106–19.
[37] Seki D, Pijet P, Wanic A. Polymer 1993;34:2440–2.
[38] Watari T, Wang H, Kuwahara K, Tanaka K, Kita H, Okamoto K. J Membr Sci 2003;219:137–47.